Higher order Rab programming in phagolysosome biogenesis

Esteban A. Roberts,[1] Jennifer Chua,[1] George B. Kyei,[1] and Vojo Deretic[1,2]

[1]Department of Molecular Genetics and Microbiology and [2]Department of Cell Biology and Physiology, University of New Mexico School of Medicine, Albuquerque, NM 87131

Phagosomes offer kinetically and morphologically tractable organelles to dissect the control of phagolysosome biogenesis by Rab GTPases. Model phagosomes harboring latex beads undergo a coordinated Rab5–Rab7 exchange, which is akin to the process of endosomal Rab conversion, the control mechanisms of which are unknown. In the process of blocking phagosomal maturation, the intracellular pathogen *Mycobacterium tuberculosis* prevents Rab7 acquisition, thus, providing a naturally occurring tool to study Rab conversion. We show that *M. tuberculosis* inhibition of Rab7 acquisition and arrest of phagosomal maturation depends on Rab22a. Four-dimensional microscopy revealed that phagosomes harboring live mycobacteria recruited and retained increasing amounts of Rab22a. Rab22a knockdown in macrophages via siRNA enhanced the maturation of phagosomes with live mycobacteria. Conversely, overexpression of the GTP-locked mutant Rab22aQ64L prevented maturation of phagosomes containing heat-killed mycobacteria, which normally progress into phagolysosomes. Moreover, Rab22a knockdown led to Rab7 acquisition by phagosomes harboring live mycobacteria. Our findings show that Rab22a defines the critical checkpoint for Rab7 conversion on phagosomes, allowing or disallowing organellar transition into a late endosomal compartment. *M. tuberculosis* parasitizes this process by actively recruiting and maintaining Rab22a on its phagosome, thus, preventing Rab7 acquisition and blocking phagolysosomal biogenesis.

Introduction

The Rab family of small GTP-binding proteins is responsible for the spatial and functional organization of intracellular compartments and controls vesicular transport between organelles in eukaryotic cells (Pereira-Leal and Seabra, 2001; Zerial and McBride, 2001; Pfeffer, 2005). The principles of Rab function as regulatory GTPases and how they control downstream processes through Rab effectors are well understood (Novick and Zerial, 1997; Zerial and McBride, 2001). Details are emerging on the coordination of the action of Rab GTPases when they function within a contiguous organelle (Sonnichsen et al., 2000; Barbero et al., 2002; de Renzis et al., 2002). Less is known about the higher level organization when a complement of Rabs functions within a complex multistage trafficking pathway.

It has been reported that maturation from early to late endosomes involves a novel process of abrupt, synchronous Rab5–Rab7 replacement on an entire early endosomal organelle (Rink et al., 2005). This process, which is termed Rab conversion, ushers the maturation of an early endosome into a late endosomal organelle (Rink et al., 2005). A functionally similar process of Rab handover seems to operate within the biosynthetic pathway in yeast (Ortiz et al., 2002). The events that govern endosomal Rab conversion are only beginning to be elucidated (Rink et al., 2005). In this context, phagolysosome biogenesis provides a convenient and morphologically tractable model system (Vergne et al., 2005). Maturing phagosomes closely mirror trafficking events observed within the endocytic pathway (Alvarez-Dominguez et al., 1996; Via et al., 1997; Vieira et al., 2003). A phagosome, when it normally matures into a phagolysosome, undergoes a transition between the stages marked by Rab5 and Rab7 (Desjardins et al., 1994; Via et al., 1997). The switch between Rab5 and Rab7 on a phagosome correlates with functional changes from an organelle with early endosomal characteristics to a compartment with lysosomal, degradative properties.

When taken up by the phagocytic cell, *Mycobacterium tuberculosis* can arrest phagosomal maturation and prevent phagolysosome biogenesis (Russell, 2001; Vergne et al., 2004), providing an advanced model system to study the role of Rabs and their effectors in phagosome maturation. Initially, Rab5 was

E.A. Roberts and J. Chua contributed equally to this paper.

Correspondence to Vojo Deretic: vderetic@salud.unm.edu

Abbreviations used in this paper: 4D, four-dimensional; BCG, bacillus Calmette-Guérin.

The online version of this article contains supplemental material.

© The Rockefeller University Press $8.00
The Journal of Cell Biology, Vol. 174, No. 7, September 25, 2006 923–929
http://www.jcb.org/cgi/doi/10.1083/jcb.200603026

identified as one of the low molecular weight GTP-binding proteins present on mycobacterial phagosomes (Via et al., 1997), leading to the identification of Rab effectors (Fratti et al., 2001) involved in mycobacterial phagosome maturation arrest. Rab7 is excluded from the *M. tuberculosis* phagosome (Via et al., 1997), indicating that mycobacterial phagosomes do not undergo Rab5–Rab7 conversion. We report that Rab22a, which is a member of the group V Rabs (Pereira-Leal and Seabra, 2001), is a key Rab, accumulating on mycobacterial phagosomes and precluding their acquisition of Rab7 and maturation into phagolysosomes.

Results and discussion

Dynamics of group V Rabs on phagosomes analyzed by quantitative four-dimensional (4D) confocal microscopy

We investigated the members of the group V Rabs (Pereira-Leal and Seabra, 2001), Rab5, Rab21, and Rab22a, by live microscopy using a previously published approach (Chua and Deretic, 2004; Vergne et al., 2005). The entry of a phagocytosed particle was identified as previously described (Chua and Deretic, 2004), and live imaging was initiated to record EGFP-Rab dynamics on nascent and maturing phagosomes containing latex beads (Fig. 1, A–C), followed by quantification using ratiometric analysis of intensities comparing phagosome and cytosol fluorescence values ($R_{\Phi/c}$; Fig. 1, G–I; Chua and Deretic, 2004; Vergne et al., 2005). The majority of the group V Rabs were transiently recruited to latex bead phagosomes (Fig. 1, A–C), with Rab5 and Rab21 (Fig. 1, A and B) desorbing from the phagosomes by 10 min after the uptake (Fig. 1, G and H), and with Rab22a showing a diminutive initial peak (Fig. 1, C and I). Because of a very low-level EGFP-Rab22a recruitment to latex bead phagosomes, we wondered whether macrophages expressed Rab22a. Rab22a expression was confirmed by RT-PCR (Fig. S1 A, available at http://www.jcb.org/cgi/content/full/jcb.200603026/DC1). In addition, endogenous

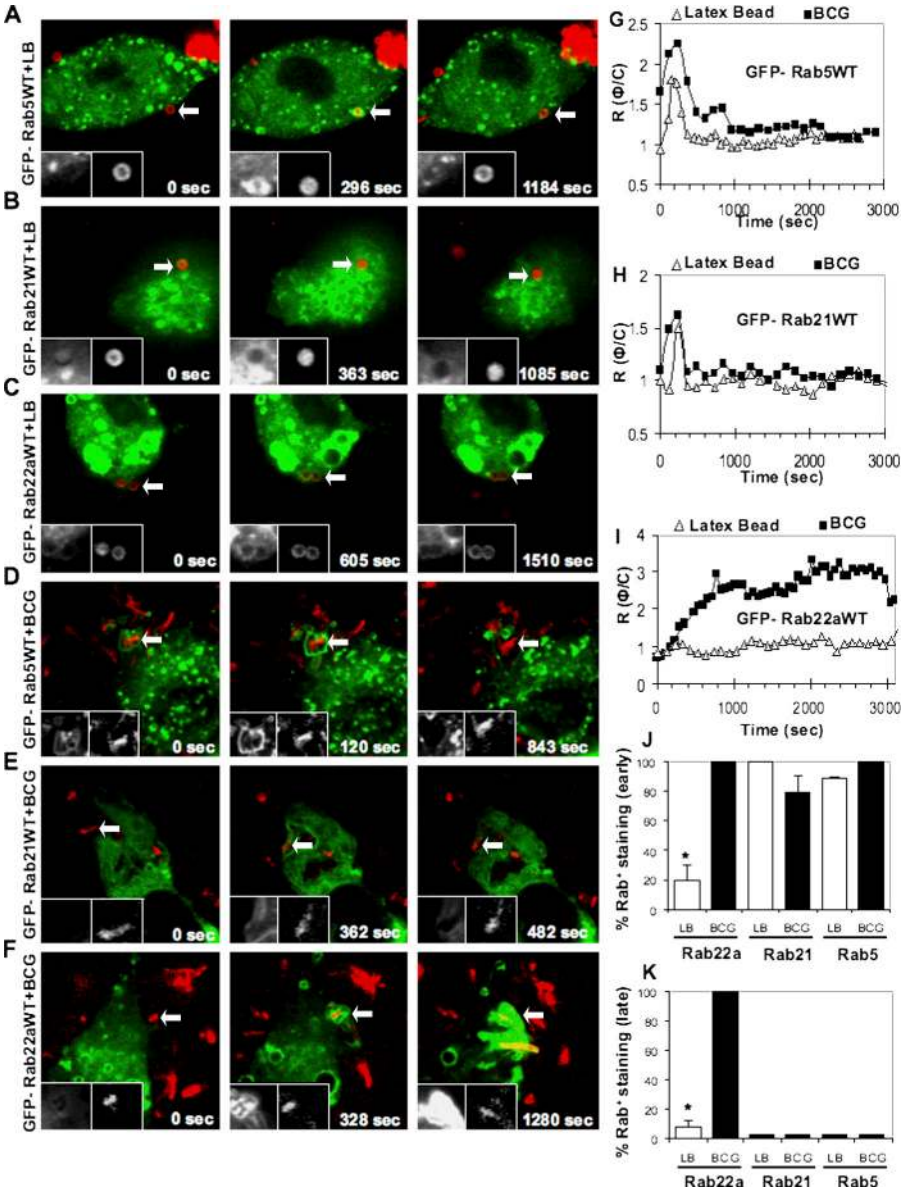

Figure 1. **Dynamics of group V Rabs on phagosomes.** RAW264.7 transfected with EGFP-Rab5WT (A and D), EGFP-Rab21WT (B and E), and EGFP-Rab22WT (C and F) were allowed to phagocytose Texas red–labeled latex beads or Texas red–labeled live *M. tuberculosis* variant *bovis* BCG. EGFP-Rab5WT (A), EGFP-Rab21WT (B), and EGFP-Rab22aWT (C) were transiently recruited to latex bead phagosomes and subsequently dissociated. EGFP-Rab5WT (D) and EGFP-Rab21WT (E) are recruited transiently on mycobacterial phagosomes and immediately dissociate. In contrast, EGFP-Rab22aWT was retained on mycobacterial phagosomes throughout the imaging period (F) of 1 h after phagocytosis. Left insets correspond to GFP fluorescence of the Rabs and the right insets correspond to the fluorescence of latex beads or mycobacteria. All microscopy imaging was performed using an UltraView LCI system. (G–I) Temporal quantification of phagosome fluorescence intensity relative to fluorescence of the cytosol. $R_{\Phi/C}$, ratio between phagosome fluorescence intensity and cytosol fluorescence intensity. Shown are $R_{\Phi/C}$ obtained by 4D microscopy and live imaging of EGFP-Rab5WT (G), EGFP-Rab21WT (H), and EGFP-Rab22aWT (I) harboring latex beads (open triangles) and live mycobacteria (filled squares). The number of phagosomes counted are as follows: EGFP-Rab5WT = 35; EGFP-Rab21WT = 24; EGFP-Rab22aWT = 47. (J) Quantification of EGFP-Rab5WT, EGFP-Rab21WT, and EGFP-Rab22aWT positivity on the latex bead phagosomes (open bars) and live mycobacterial phagosomes (filled bars) during the first 10 min after phagocytosis. *, $P = 0.0002$. (K) Quantification of EGFP-Rab5WT, EGFP-Rab21WT, and EGFP-Rab22aWT positivity on the latex bead phagosomes (open bars) and live mycobacterial phagosomes (filled bars) 45 min after phagocytosis. *, $P < 0.0001$.

Rab22a was detected in macrophages by immunofluorescence (Fig. S1 B). Hence, low levels of Rab22a on latex bead phagosomes cannot be explained by a lack of Rab22a expression in macrophages. Thus, the group V Rabs are transiently recruited in small amounts to latex bead phagosomes during early time points after phagocytosis.

Mycobacterial phagosomes recruit and retain copious amounts of Rab22a

We next tested group V Rab dynamics on mycobacterial phagosomes. Rab5 and Rab21 followed similar kinetics on both mycobacterial and latex beads phagosomes (Fig. 1, D and E, G and H). However, mycobacterial phagosomes displayed a marked difference relative to latex bead phagosomes by recruiting and retaining high quantities of Rab22a (Fig. 1, F and I). Enumeration of Rab5, Rab21, and Rab22a profiles (Fig. 1, J and K) confirmed that Rab22a was persistently accumulating on mycobacterial phagosomes. This was accompanied by diminishing levels of EGFP-Rab22aWT fluorescence in other parts of the cell, a phenomenon that was augmented in macrophages infected with more than one bacillus. EGFP-Rab22aWT–positive profiles were observed to tether and fuse with mycobacterial phagosomes, increasing EGFP-Rab22aWT levels on these organelles (Video 1, available at http://www.jcb.org/cgi/content/full/jcb.200603026/DC1). These observations were confirmed by immunofluorescence detection of endogenous Rab22a on bacillus Calmette-Guérin (BCG) phagosomes (Fig. S1 B). The differential distribution of EGFP-Rab22aWT was not caused by phagosome size difference because 3-μm latex beads (Fig. S1 C) behaved similarly to the 1-μm beads. Thus, Rab22a is specifically enriched on phagosomes containing mycobacteria.

Rab22a is an early endocytic Rab in macrophages

Rab22a has been implicated in early endosomal and recycling pathways in nonphagocytic cells (Kauppi et al., 2002; Weigert et al., 2004). We tested Rab22a localization in macrophages and found that both EGFP-Rab22aWT and endogenous Rab22a overlapped with the early endosomal marker EEA1 (Fig. S1, D and E). This is in keeping with the reported early endosomal localization of Rab22a in other cells (Kauppi et al., 2002). Immunofluorescence analysis using GM130, syntaxin 6, and TGN38 showed that in macrophages Rab22a was not on Golgi organelles (Fig. S1 F), and Golgi vesiculation did not occur in cells transfected with EGFP-Rab22aQ64L (Fig. S1 F), in contrast to a report that the Rab22a mutant vesiculates Golgi in CHO cells (Kauppi et al., 2002). The early endosomal localization of Rab22a, and the increased fusion of early endosomal organelles with mycobacterial phagosomes stimulated by Rab14 (unpublished data), may partially explain Rab22a enrichment on BCG phagosomes.

Rab22a affects phagosomal maturation

We examined whether expression of constitutively active Rab22a (EGFP-Rab22aQ64L) affected phagosomes harboring dead mycobacteria. Heat inactivation of *M. tuberculosis* incapacitates it to block phagolysosome biogenesis (Armstrong and Hart, 1971; Chua and Deretic, 2004; Vergne et al., 2005). The constitutively active mutant of Rab22a accumulates on mycobacterial phagosomes (Fig. S1 G) in a manner similar to wild-type Rab22a. Expression of EGFP-Rab22aQ64L inhibited maturation of phagosomes containing dead BCG, as follows: (a) heat-killed BCG phagosomes showed reduced colocalization with the acidotropic dye LysoTracker Blue (Fig. 2, A–F), indicating impaired acidification; (b) phagosomes with dead BCG showed lower proteolytic activity in macrophages transfected with EGFP-Rab22aQ64L, as indicated by lower staining with DQ-Red BSA, which is an endocytic protease substrate whose fluorescence dequenches upon proteolysis (Fig. 2, G–L); (c) although phagosomes harboring dead mycobacteria normally do not retain transferrin receptor (Fig. 3, A–D and Q), transfection with EGFP-Rab22aQ64L caused significant presence of transferrin receptor on dead mycobacterial phagosomes (Fig. 3, E–H and Q); (d) A similar effect was observed

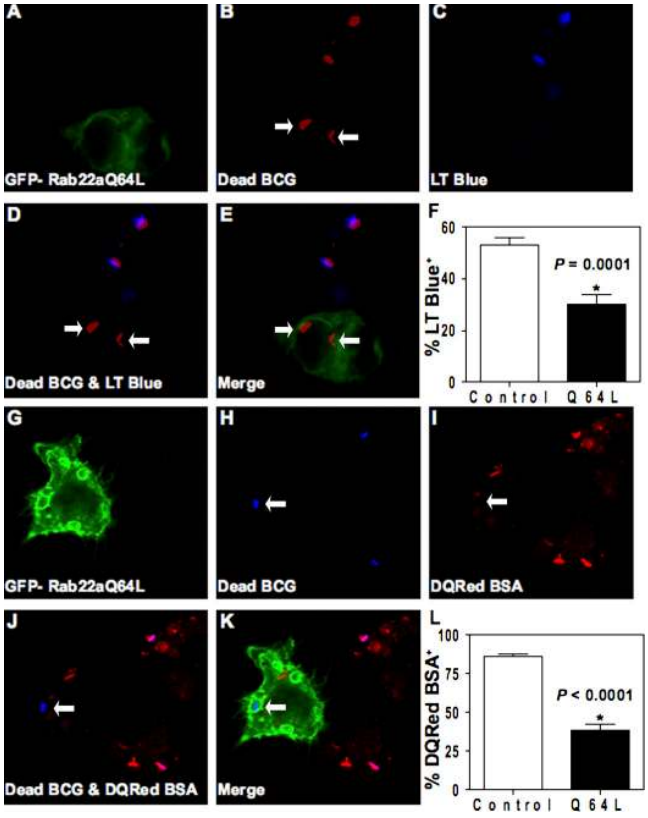

Figure 2. **Constitutively active Rab22aQ64L prevents normal maturation of phagosomes harboring dead mycobacterial phagosomes.** RAW264.7 cells were transfected with EGFP-Rab22aQ64L and infected with dead mycobacteria in the presence of Lysotracker Blue (A–E) or DQ Red BSA (G–K). A and G show fluorescence from GFP. B and H show the fluorescence of dead mycobacteria labeled with Texas red and Alexa Fluor 647, respectively. C and I show the fluorescence of Lysotracker Blue (blue) and DQ Red BSA (red), respectively. D shows the merge image of mycobacteria (red) and Lysotracker Blue (blue). J shows the merge image of mycobacteria (blue) and DQ Red BSA (red). E and K represent RGB composite images. Arrows indicate no colocalization between dead mycobacterial phagosomes and probes in EGFP-Rab22aQ64L–expressing cells. (F) Quantification of Lysotracker Blue staining on dead mycobacterial phagosomes in control versus EGFP-Rab22aQ64L–expressing cells. $P = 0.0001$. (L) Quantification of DQ Red BSA staining on dead mycobacterial phagosomes in control versus EGFP-Rab22aQ64L–expressing cells. *, $P < 0.0001$.

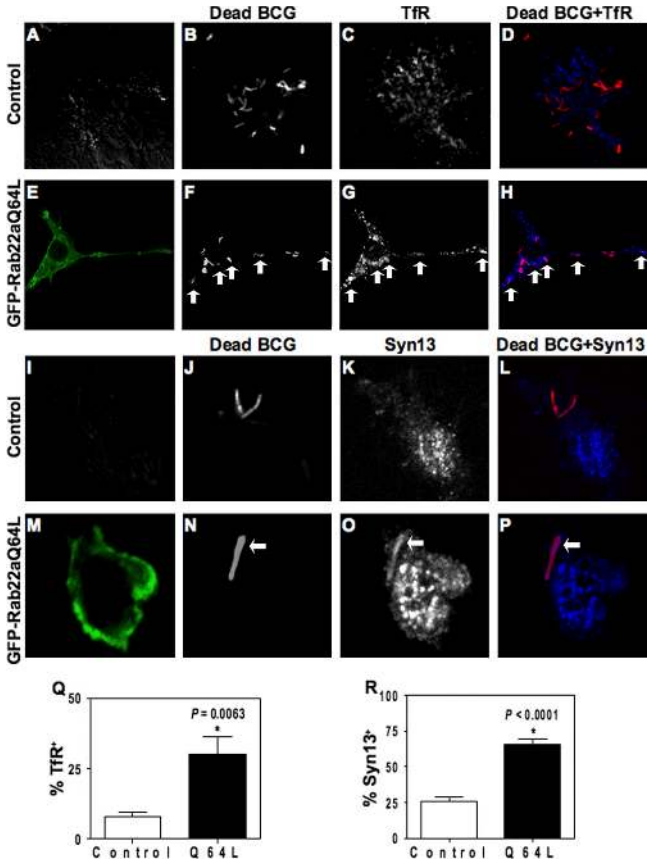

Figure 3. **EGFP-Rab22aQ64L confers recycling endosomal characteristics on dead mycobacterial phagosomes.** Nontransfected RAW264.7 cells (A–D and I–L) and EGFP-Rab22aQ64L–expressing cells (E–H and M–P) were infected with dead mycobacteria and immunostained for TfR (A–H) and syntaxin 13 (I–P). Anti-TfR antibodies did not stain dead mycobacterial phagosomes (A–D) in control cells, whereas staining can be seen in EGFP-Rab22aQ64L–expressing cells (E–H). Anti-syntaxin 13 antibodies also did not stain dead mycobacterial phagosomes in control cells (I–L), but stained in EGFP-Rab22aQ64L–transfected cells (M–P). (Q) Quantification of TfR-positive dead mycobacterial phagosomes. *, $P = 0.0063$. (R) Quantification of syntaxin13–positive dead mycobacterial phagosomes. *, $P < 0.0001$.

with another previously mapped (Fratti et al., 2003b) early/recycling endocytic marker, syntaxin 13 (Fig. 3, I–P and R); and (e) Rab11, a GTPase that controls transferrin receptor (TfR) recycling (Ullrich et al., 1996; Ren et al., 1998), accumulated on dead mycobacterial phagosomes in cells expressing EGFP-Rab22aQ64L when compared with control untransfected cells ($34 \pm 5\%$ vs. $14 \pm 4\%$ colocalization; $P = 0.04$; Fig. S1 H), indicating that the constitutively active mutant of Rab22a conferred recycling endosomal characteristics upon dead mycobacterial phagosomes.

Knockdown of Rab22a overcomes the mycobacterial phagosome maturation block

In lieu of experiments with a dominant-negative Rab22a, which was found to cause macrophage detachment, we resorted to siRNA knockdown of Rab22a and examined its effects on maturation of phagosomes harboring live *M. tuberculosis* variant *bovis* BCG. Rab22a knockdown (Fig. 4 A) caused a threefold increase in the colocalization of live mycobacterial phagosomes with the most robust late endocytic marker CD63 (Fig. 4, B and E; Fratti et al., 2003b), indicating that live mycobacterial phagosomes were maturing into phagosomes with late endosomal characteristics. Live mycobacterial phagosomes also showed a doubling of V_o H^+ATPase association with phagosomes containing live mycobacteria (Fig. 4, C and F; Sturgill-Koszycki et al., 1994; Fratti et al., 2003b). Rab22a knockdown did not cause indiscriminate mixing of endosomal markers (Fig. S2, A–C, available at http://www.jcb.org/cgi/content/full/jcb.200603026/DC1). Furthermore, colocalization of TfR with live mycobacterial phagosomes was diminished upon Rab22a siRNA knockdown compared with scrambled siRNA control (Fig. 4, D and G).

The effects of Rab22a knockdown with SMARTpool (Dharmacon) Rab22a siRNA (a combination of four Rab22a-specific siRNA duplexes) was confirmed using individual siRNA duplexes (Fig. S2 D), which also caused an increase in live mycobacterial phagosome maturation (Fig. S3, A–D, available at http://www.jcb.org/cgi/content/full/jcb.200603026/DC1). Furthermore, transfection with siRNA against the closely related Rab22b, which is also expressed in macrophages (Fig. S2, E and F), did not alter mycobacterial phagosomes (Fig. S3, A–D). The effects of Rab22a knockdown on mycobacterial survival (Fig. S3, E–G) were mild within the period investigated, and although a trend was observed, no statistically significant differences could be established (Fig. S3, F and G). We conclude that Rab22a is necessary to maintain *M. tuberculosis* phagosome maturation block, but that maturation block override does not automatically translate into direct bacterial elimination by macrophages, in keeping with the early observations by Armstrong and Hart (1975).

Rab22a knockdown leads to Rab7 conversion on *M. tuberculosis* phagosomes

A prequel to endosomal maturation into late endosomal/lysosomal organelles is Rab conversion (Rink et al., 2005). This term describes a process whereby an organelle synchronously sheds off early endosomal Rab(s) and concomitantly receives the late endosomal Rab, Rab7 (Rink et al., 2005). The signals for this transition are currently unknown (Deretic, 2005). We wondered whether Rab conversion applies to phagosomes, and whether Rab22a, as a candidate terminal recycling Rab involved in cargo and membrane sorting from the early endosome (Mesa et al., 2001; Weigert et al., 2004), could supply or contribute to such signals. To test this, we examined Rab7 acquisition by the mycobacterial phagosome, which was previously shown to exclude this critical late endocytic Rab (Via et al., 1997). Unlike in cells treated with control scrambled siRNA, Rab7 acquisition was increased to 80% on live mycobacterial phagosomes in macrophages in which Rab22a was knocked down by siRNA (Fig. 5). These findings are consistent with a functional role for Rab22a in mycobacterial phagosome maturation block. More generally, the conversion of live mycobacterial phagosomes into the Rab7 stage upon Rab22a knockdown suggests that Rab22a supplies signals preventing acquisition of Rab7 and precluding organellar maturation into a late endosomal/lysosomal

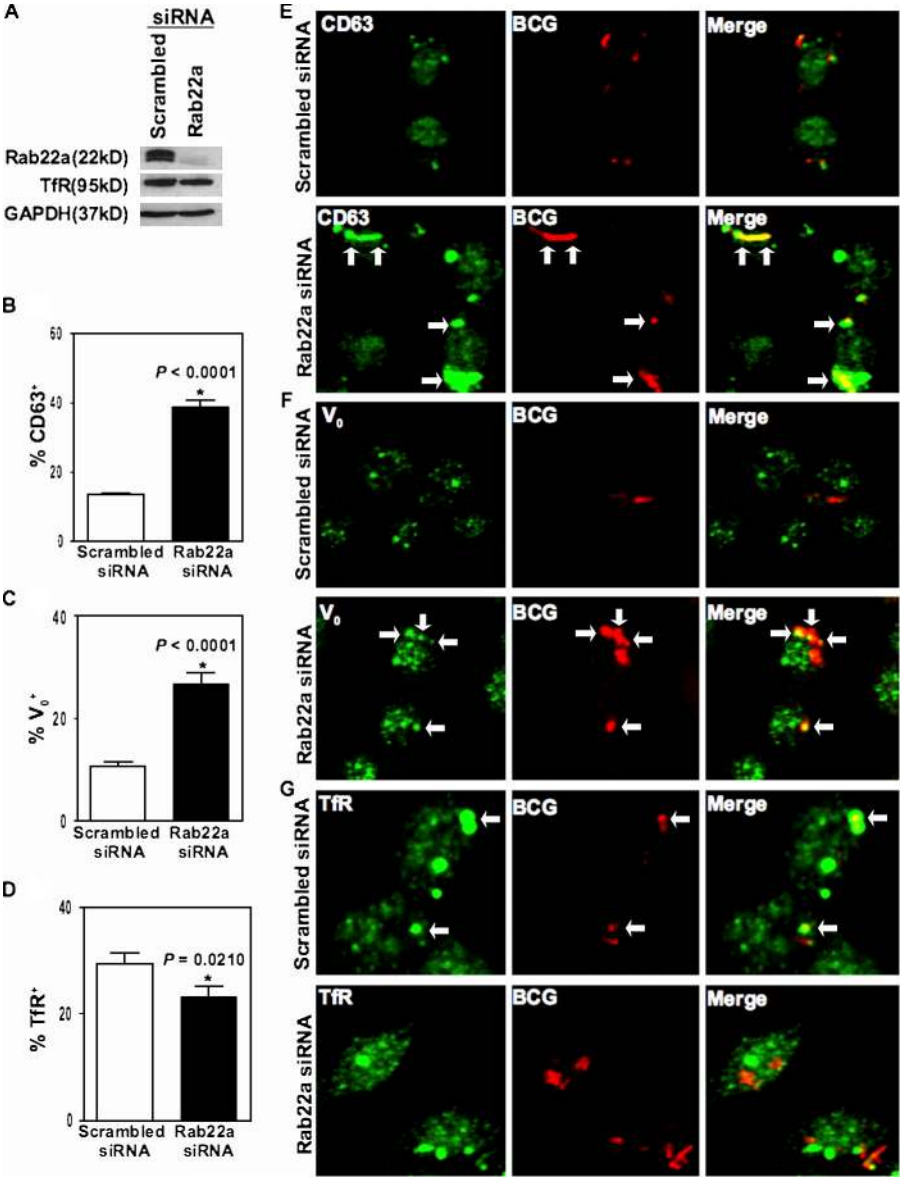

Figure 4. **Rab22a knockdown promotes the maturation of phagosomes with live mycobacteria.** RAW264.7 macrophages were transfected with siRNA to Rab22a for 24 h and lysates probed for endogenous Rab22a knockdown via immunoblotting (A). There was no observable effect on the levels of TfR by Rab22a knockdown (A). RAW264.7 macrophages were transfected with siRNA to Rab22a for 24 h to provide sufficient suppression of Rab22a expression and subsequently infected with Texas red–labeled live *M. tuberculosis* variant *bovis* BCG for 10 min, followed by a 1-h chase period. Although only 13% of live mycobacterial phagosomes colocalize with CD63-positive compartments in macrophages transfected with scrambled siRNA (B and E), 40% of live mycobacterial phagosomes were positive for CD63 colocalization in cells transfected with Rab22a siRNA (B and E). Similarly, Rab22a siRNA–mediated inhibition enhanced the colocalization of live mycobacterial phagosomes with V_0-positive compartments (C and F) by 2.8-fold when compared with minimal phagosomal colocalization in scrambled siRNA–transfected cells (C and F). Rab22a siRNA significantly inhibited the colocalization of Texas red–labeled live *M. tuberculosis* variant *bovis* BCG phagosomes with TfR (D and G) compared with scrambled siRNA (D and G). These results demonstrate that Rab22a is essential for mycobacterial ability in maintaining an immature phagosomal niche.

compartment. Thus, Rab22a functions not only as a recycling Rab involved in cargo and membrane sorting from the early endosome (Mesa et al., 2001; Weigert et al., 2004), but it also acts as a coordinator of Rab succession. In keeping with our findings with phagosomes, there is a lack of endosomal EGF degradation in Rab22aQ64L-transfected Hep2 cells (Kauppi et al., 2002). In CHO cells, the expression of Rab22aQ64L causes endocytic tracers to remain in Rab22a-positive vesicles

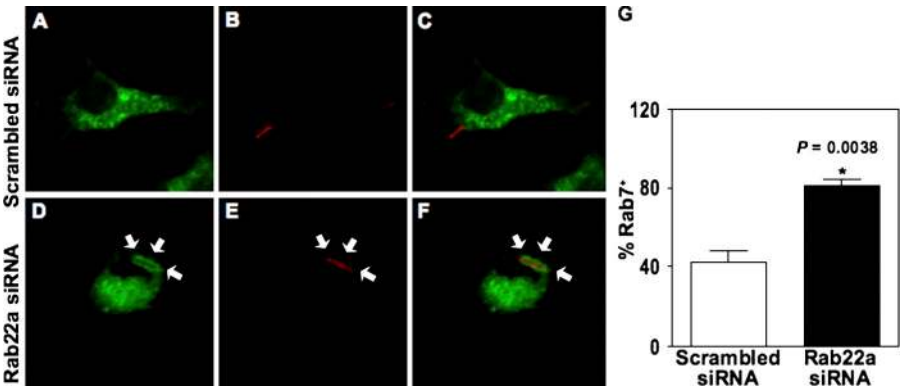

Figure 5. **Rab7 acquisition by phagosomes is dependent on Rab22a.** Rab22a knockdown in RAW264.7 macrophages led to increased late endosomal GTPase Rab7 recruitment to live mycobacterial phagosomes (D–F and G) compared with macrophages transfected with scrambled siRNA (A–C and G).

(Mesa et al., 2005). We propose that Rab22a is a central regulator of the transition to late endocytic organelles by signaling "all clear" and allowing the leftover sorting endosomal or phagosomal organelle to transit from an early compartment to a degradative organelle controlled by Rab7.

Materials and methods

Cell culture and preparation of Texas red–labeled latex beads and *M. tuberculosis* variant *bovis* BCG

RAW264.7 macrophages and *M. tuberculosis* variant *bovis* BCG were maintained as previously described (Chua and Deretic, 2004). Mycobacteria were heat killed by incubation at 90°C for 5 min before labeling. Both live and dead mycobacteria were labeled with 0.5 mg/ml Texas red–succinimidyl ester and prepared as previously described (Chua and Deretic, 2004). Dead mycobacteria were also labeled with 0.25 mg/ml Alexa Fluor 647–succinimidyl ester in PBS for 1 h. Streptavidin-conjugated 1-μm polystyrene beads (Sigma-Aldrich) were labeled and prepared as previously described (Chua and Deretic, 2004). 3-μm polystyrene beads were opsonized in DME supplemented with 10% FBS before use.

Plasmids and transfection

The plasmids pEGFP-Rab21WT, pEGFP-Rab22aWT, and pEGFP-Rab22aQ64L were obtained from J. Donaldson (National Institutes of Health, Bethesda, MD), pEGFP-hRab5WT was obtained from P. Stahl (Washington University, St. Louis, MO), and pEGFP-Rab7WT was obtained from A. Wandinger-Ness (University of New Mexico, Albuquerque, NM). For transfection, 5×10^6 RAW264.7 cells were resuspended in a nucleoporator buffer supplied by the manufacturer (Amaxa Biosystems) with 5 μg of plasmid DNA. Cells were nucleoporated according to the manufacturer's protocol and allowed to express the construct for 24 h before the imaging experiments.

Antibodies and endocytic tracers

Rabbit polyclonal antibody to Rab22a was obtained from J. Donaldson, and polyclonal antibody to syntaxin 13 was obtained from R. Scheller (Genentech, South San Francisco, CA). Rabbit polyclonal antibodies to transferrin receptor and CD63 were purchased from Santa Cruz Biotechnology, Inc. Antibody to V_0 was used as previously described (Fratti et al., 2003a,b). Mouse monoclonal antibody to transferrin receptor was purchased from Zymed Laboratories. Monoclonal antibodies against GAPDH, GM130, and TGN38 were obtained from Abcam. Lysotracker Blue, DQ Red BSA, and secondary antibodies conjugated to Alexa Fluor 488, 568, and 647 were purchased from Invitrogen. The acidotropic dye Lysotracker Blue was diluted in DME (1:10,000) and preloaded into macrophages for 2 h. DQ Red BSA was preloaded at 10 μg/ml for 3 h before infection. Cells were subsequently fixed and viewed using immunofluorescence microscopy.

Rab siRNA knockdowns and immunoblotting

Rab22a and Rab22b knockdowns were achieved by using siGENOME SMARTpool reagent (Dharmacon) specific for *Mus musculus* Rab22a and Rab22b (Dharmacon). All effects of Rab siRNAs were compared with siCONTROL Nontargeting siRNA pool (Dharmacon), which is labeled as scrambled siRNA in figures. RAW264.7 cells were transfected with 1.5 μg siRNA by nucleoporation. Immunoblotting (30 μg of total protein) was performed as previously described (Fratti et al., 2003a,b). GAPDH immunoblotting was used as a loading control. Rab22a single siRNA duplexes used individually were as follows: duplex 1, sense (CAGCAGCCAUCAUCAUCGUUUAUU) and antisense (5′-PUAAACGAUGAUGAUGGCUGCUGUU); duplex 2, sense (GGGAACAAGUGCGAUCUUAUU) and antisense (5′-PUAAGAUCGCACUUGUUCCCUU); duplex 3, sense (GAGAUUAGUCGAAGAAUUCUU) and antisense (5′-PGAAUUCUUCGAAGAAUUCUU); and duplex 4, sense (GGAUACGGGUGUGGGUAAAUU) and antisense (5′-PUUUACCCACACCCGUAUCCUU).

Immunofluorescence laser scanning confocal microscopy

Imaging of 1-μm-thick optical sections was performed using an Axiovert 200M microscope with an Axioscope 63× oil objective and LSM 5 Pascal or LSM 510 META systems (Carl Zeiss MicroImaging, Inc.). At least 200 phagosomes from three independent experiments were analyzed for colocalization studies.

4D confocal microscopy

A rotating disk confocal microscope (UltraView; PerkinElmer) that affords low photocytotoxicity and low photobleaching was applied for 4D imaging, as previously described (Chua and Deretic, 2004; Vergne et al., 2005). For ratiometric quantitative analysis (Chua and Deretic, 2004; Vergne et al., 2005) of a volume over time, z sections were collapsed into a single projection according to the published procedure (Gerlich et al., 2001). Transfected RAW264.7 cells were synchronously infected by centrifugation of bacteria or beads onto macrophages adherent to coverslips at 1,000 rpm for 5 min. Coverslips were mounted into a perfusion chamber (Harvard Apparatus) set at 37°C. Identification of mycobacterial entry and image acquisition was performed as previously described (Chua and Deretic, 2004). To measure $R_{\Phi/C}$, fluorescence intensity of the phagosomal membrane was divided by background cytosolic fluorescence.

Mycobacterial survival assay

RAW264.7 macrophages were seeded at 2.0×10^5 cells/well in 12-well plates after transfection with either siGENOME SMARTpool Rab22a siRNA or scrambled siRNA. Cells were incubated for 24 h. Macrophages were infected with live *M. tuberculosis* variant *bovis* BCG or live *M. tuberculosis* H37Rv (preincubated for 30 min at 37°C in DME), at a nominal multiplicity of infection of 10, followed by four washes using complete DME. Macrophages were hypotonically lysed using cold sterile water after a 2, 4, or 24 h chase period. Mycobacteria were plated for colony forming units on Middlebrook 7H11 agar (Difco) and incubated at 37°C for 2.5 wk. Bacterial viability was expressed as percentage of survival relative to scrambled siRNA control. Experiments were performed in triplicate.

Statistical analysis

Results are from experiments performed in triplicate. All statistical analyses were calculated using Fisher's protected least significant difference post hoc test (analysis of variance, ANOVA) (SuperANOVA 1.11; Abacus Concepts). P values of ≤ 0.05 were considered significant.

Online supplemental material

Fig. S1 shows that endogenous Rab22a and EGFP-Rab22aQ64L in macrophages is recruited to mycobacterial phagosomes and that Rab22a colocalizes with early endosomes, but not Golgi organelles. Fig. S2 shows an analysis of Rab22a knockdown effects on early and late endosomes, characterization of single duplex Rab22a siRNA knockdowns, and expression of Rab22b. Fig. S3 shows the effects of single-duplex siRNA Rab22a knockdown on mycobacterial phagosomal maturation and Rab22a knockdown on intracellular survival of mycobacteria. Video 1 shows an EGFP-Rab22aWT–transfected macrophage infected with live Texas red–labeled *M. tuberculosis* variant *bovis* BCG.

We thank J. Donaldson and R. Weigert for Rab22a plasmid constructs and antibody and J. Harris for assistance with siRNA experiments. E.A. Roberts was a Heiser Foundation Postdoctoral Fellow in Tuberculosis and Leprosy Research.

This work was supported by grant AI45148 from the National Institutes of Health.

Submitted: 6 March 2006
Accepted: 17 August 2006

References

Alvarez-Dominguez, C., A.M. Barbieri, W. Beron, A. Wandinger-Ness, and P.D. Stahl. 1996. Phagocytosed live *Listeria monocytogenes* influences Rab5-regulated in vitro phagosome-endosome fusion. *J. Biol. Chem.* 271:13834–13843.

Armstrong, J.A., and P.D. Hart. 1971. Response of cultured macrophages to *Mycobacterium tuberculosis*, with observations on fusion of lysosomes with phagosomes. *J. Exp. Med.* 134:713–740.

Armstrong, J.A., and P.D. Hart. 1975. Phagosome-lysosome interactions in cultured macrophages infected with virulent tubercle bacilli. Reversal of the usual nonfusion pattern and observations on bacterial survival. *J. Exp. Med.* 142:1–16.

Barbero, P., L. Bittova, and S.R. Pfeffer. 2002. Visualization of Rab9-mediated vesicle transport from endosomes to the trans-Golgi in living cells. *J. Cell Biol.* 156:511–518.

Chua, J., and V. Deretic. 2004. Mycobacterium tuberculosis reprograms waves of phosphatidylinositol 3-phosphate on phagosomal organelles. *J. Biol. Chem.* 279:36982–36992.

de Renzis, S., B. Sonnichsen, and M. Zerial. 2002. Divalent Rab effectors regulate the sub-compartmental organization and sorting of early endosomes. *Nat. Cell Biol.* 4:124–133.

Deretic, V. 2005. Ay, there's the rab: organelle maturation by Rab conversion. *Dev. Cell*. 9:446–448.

Desjardins, M., L.A. Huber, R.G. Parton, and G. Griffiths. 1994. Biogenesis of phagolysosomes proceeds through a sequential series of interactions with the endocytic apparatus. *J. Cell Biol.* 124:677–688.

Fratti, R.A., J.M. Backer, J. Gruenberg, S. Corvera, and V. Deretic. 2001. Role of phosphatidylinositol 3-kinase and Rab5 effectors in phagosomal biogenesis and mycobacterial phagosome maturation arrest. *J. Cell Biol.* 154:631–644.

Fratti, R.A., J. Chua, and V. Deretic. 2003a. Induction of p38 mitogen-activated protein kinase reduces early endosome autoantigen 1 (EEA1) recruitment to phagosomal membranes. *J. Biol. Chem.* 278:46961–46967.

Fratti, R.A., J. Chua, I. Vergne, and V. Deretic. 2003b. Mycobacterium tuberculosis glycosylated phosphatidylinositol causes phagosome maturation arrest. *Proc. Natl. Acad. Sci. USA*. 100:5437–5442.

Gerlich, D., J. Beaudouin, M. Gebhard, J. Ellenberg, and R. Eils. 2001. Four-dimensional imaging and quantitative reconstruction to analyse complex spatiotemporal processes in live cells. *Nat. Cell Biol.* 3:852–855.

Kauppi, M., A. Simonsen, B. Bremnes, A. Vieira, J. Callaghan, H. Stenmark, and V.M. Olkkonen. 2002. The small GTPase Rab22 interacts with EEA1 and controls endosomal membrane trafficking. *J. Cell Sci.* 115:899–911.

Mesa, R., J. Magadan, A. Barbieri, C. Lopez, P.D. Stahl, and L.S. Mayorga. 2005. Overexpression of Rab22a hampers the transport between endosomes and the Golgi apparatus. *Exp. Cell Res.* 304:339–353.

Mesa, R., C. Salomon, M. Roggero, P.D. Stahl, and L.S. Mayorga. 2001. Rab22a affects the morphology and function of the endocytic pathway. *J. Cell Sci.* 114:4041–4049.

Novick, P., and M. Zerial. 1997. The diversity of Rab proteins in vesicle transport. *Curr. Opin. Cell Biol.* 9:496–504.

Ortiz, D., M. Medkova, C. Walch-Solimena, and P. Novick. 2002. Ypt32 recruits the Sec4p guanine nucleotide exchange factor, Sec2p, to secretory vesicles; evidence for a Rab cascade in yeast. *J. Cell Biol.* 157:1005–1015.

Pereira-Leal, J.B., and M.C. Seabra. 2001. Evolution of the Rab family of small GTP-binding proteins. *J. Mol. Biol.* 313:889–901.

Pfeffer, S.R. 2005. Structural clues to Rab GTPase functional diversity. *J. Biol. Chem.* 280:15485–15488.

Ren, M., G. Xu, J. Zeng, C. De Lemos-Chiarandini, M. Adesnik, and D.D. Sabatini. 1998. Hydrolysis of GTP on rab11 is required for the direct delivery of transferrin from the pericentriolar recycling compartment to the cell surface but not from sorting endosomes. *Proc. Natl. Acad. Sci. USA*. 95:6187–6192.

Rink, J., E. Ghigo, Y. Kalaidzidis, and M. Zerial. 2005. Rab conversion as a mechanism of progression from early to late endosomes. *Cell*. 122:735–749.

Russell, D.G. 2001. *Mycobacterium tuberculosis*: here today, and here tomorrow. *Nat. Rev. Mol. Cell Biol.* 2:569–577.

Sonnichsen, B., S. De Renzis, E. Nielsen, J. Rietdorf, and M. Zerial. 2000. Distinct membrane domains on endosomes in the recycling pathway visualized by multicolor imaging of Rab4, Rab5, and Rab11. *J. Cell Biol.* 149:901–914.

Sturgill-Koszycki, S., P.H. Schlesinger, P. Chakraborty, P.L. Haddix, H.L. Collins, A.K. Fok, R.D. Allen, S.L. Gluck, J. Heuser, and D.G. Russell. 1994. Lack of acidification in *Mycobacterium* phagosomes produced by exclusion of the vesicular proton-ATPase. *Science*. 263:678–681.

Ullrich, O., S. Reinsch, S. Urbe, M. Zerial, and R.G. Parton. 1996. Rab11 regulates recycling through the pericentriolar recycling endosome. *J. Cell Biol.* 135:913–924.

Vergne, I., J. Chua, H.H. Lee, M. Lucas, J. Belisle, and V. Deretic. 2005. Mechanism of phagolysosome biogenesis block by viable *Mycobacterium tuberculosis*. *Proc. Natl. Acad. Sci. USA*. 102:4033–4038.

Vergne, I., J. Chua, S.B. Singh, and V. Deretic. 2004. Cell biology of *mycobacterium tuberculosis* phagosome. *Annu. Rev. Cell Dev. Biol.* 20:367–394.

Via, L.E., D. Deretic, R.J. Ulmer, N.S. Hibler, L.A. Huber, and V. Deretic. 1997. Arrest of mycobacterial phagosome maturation is caused by a block in vesicle fusion between stages controlled by rab5 and rab7. *J. Biol. Chem.* 272:13326–13331.

Vieira, O.V., C. Bucci, R.E. Harrison, W.S. Trimble, L. Lanzetti, J. Gruenberg, A.D. Schreiber, P.D. Stahl, and S. Grinstein. 2003. Modulation of Rab5 and Rab7 recruitment to phagosomes by phosphatidylinositol 3-kinase. *Mol. Cell. Biol.* 23:2501–2514.

Weigert, R., A.C. Yeung, J. Li, and J.G. Donaldson. 2004. Rab22a regulates the recycling of membrane proteins internalized independently of clathrin. *Mol. Biol. Cell*. 15:3758–3770.

Zerial, M., and H. McBride. 2001. Rab proteins as membrane organizers. *Nat. Rev. Mol. Cell Biol.* 2:107–117.